

Shifts and dips in inelastic-electron-tunneling spectra due to the tunnel-junction environment

A. Bayman and P. K. Hansma

Department of Physics, University of California, Santa Barbara, California 93106

W. C. Kaska

Department of Chemistry, University of California, Santa Barbara, California 93106

(Received 30 January 1981)

In general, the tunnel-junction environment has proved to be surprisingly benign; tunneling spectra of molecules included within tunnel junctions are similar to infrared and Raman spectra of molecules not covered by a metal electrode. Peak shifts have been typically less than the linewidth of the peaks, and peak intensities have been comparable to infrared and Raman intensities. Here we report a different situation for tunnel junctions containing molecules adsorbed on metal particles. Specifically, we find that different-top-metal electrodes give different tunneling spectra for CO on alumina-supported iron and rhodium particles. Though metals with similar atomic radii give similar spectra, metals with dissimilar atomic radii can give qualitatively different spectra. We also find anomalies concerning intensities. Specifically, for methyl isocyanide adsorbed on alumina-supported rhodium particles, the strongest peak in the infrared spectrum, the $\text{-N}\equiv\text{C}$ stretching mode, appears as a *dip* in the tunneling spectrum.

I. INTRODUCTION

Inelastic-electron-tunneling spectroscopy reveals the vibrational modes of organic molecules on the oxide of a metal-oxide-metal junction.^{1,2} At a junction temperature of 4.2 K, both infrared- and Raman-active vibrational modes can be observed with a resolution of 15 to 30 cm^{-1} (about 2 to 4 meV) over a range of frequencies from 0 to 4000 cm^{-1} (0 to 500 meV).

Since its discovery,³ inelastic-electron-tunneling spectroscopy has been used in the studies of adhesion,⁴⁻⁶ biochemistry,^{7,8} water pollution,⁹ electron beam irradiation,¹⁰ uv irradiation,¹¹ and lubrication.¹² Particularly promising applications have been in surface science and catalysis.¹³⁻¹⁶

The study of the bonding and hydrogenation of carbon monoxide on alumina-supported metals is of interest. The observation of catalytic intermediates on supported metal catalysts would lead to understanding the step-by-step formation of hydrocarbons from carbon monoxide. Inelastic tunneling spectroscopy can present information on these systems similar to other vibrational spectroscopies. Hence, it is desirable to compare tunneling results with those obtained by other techniques.

It is important, however, to understand the effect of the tunnel junction environment on the measured vibrational spectra. In particular, what is the effect of the top metal electrode and what is the relationship of peak intensities to those measured by other techniques?

Kirtley and Hansma studied the effect of the top metal electrode on the peak positions and bandwidths of hydroxyl and deuterioxyl stretch bands with Pb, Sn, Ag, Au top electrodes¹⁷ and on peak positions of benzoic acid with Pb, Sn, Ag top metal electrodes.¹⁸ They observed that the peak positions are downshifted for the top metal electrodes that have the smaller atomic radii. The shifts are approximately 15 meV for O-H vibrations, 0.5 meV for C-H vibrations, and less than 0.2 meV for C-C ring stretch and bending modes.

Here we study the effect of the top metal electrode on the vibrational modes of CO bonded to Fe or Rh with Pb, Tl, Sn, In, Ag, and Au top electrodes and find more dramatic effects. We also study the effect on the hydrocarbon vibrational modes of methyl isocyanide, an electronic analog of CO. The metal-carbon vibrational region shows differences among spectra taken with Pb, Tl, Sn top electrodes; however, the hydrocarbon vibrations are shifted by less than 1% from the infrared values. Not only the peak positions but also tunneling intensities are sensitive to the junction environment.

A good deal of theoretical and experimental work has been done on the peak intensities in tunneling spectroscopy.¹⁹⁻²⁹ Kirtley and Hall²⁹ recently made a detailed comparison between theoretical calculations based on a transfer Hamiltonian theory²² and experimental results on a well characterized system. They showed that the intensities for this system can be interpreted and that the ratios of intensities give orientational information. In general, the theories predict

and experiments find that intense peaks in infrared or Raman spectra are also large in tunneling spectra. Peaks that are small or absent in *both* infrared and Raman spectra are small or absent in tunneling spectra.³⁰

Here we show results that are strikingly different. For methyl isocyanide (CH_3NC) adsorbed on rhodium particles, the largest peak in the infrared spectrum corresponds to a *dip* in the tunneling spectrum. Though general theories of tunneling intensities^{23–28} allow for the possibility of a dip, none had been observed to date. The most successful theory of tunneling intensities, the transfer Hamiltonian theory²² does not, in its present form, include the possibility of dips.

II. EXPERIMENTAL METHODS

The techniques used in this experiment differ from those contained in review articles^{1,2} only in the doping of the tunneling junctions and in the use of several top metal electrodes. Hence, we give details of these techniques and only an outline of the rest.

We evaporated an aluminum strip 700 Å thick onto a clean glass slide and partially oxidized the strip in air at 200 °C to form the alumina insulating barrier. Prior to the catalyst metal evaporation we cleaned the slide in an argon glow discharge³¹ and chilled it in a vacuum of 10^{-6} Pa (7.5×10^{-9} torr) with a liquid-nitrogen cold finger to approximately 150 K.

For the CO-doped junctions, we maintained a pressure of 7×10^{-4} Pa of CO during the evaporation of Fe and a pressure of 3×10^{-5} Pa of CO during the evaporation of Rh. We warmed the slide to room temperature before the evaporation of Pb, In, and Tl top metal electrodes. Metals that have high boiling temperatures (Sn, Ag, Au) required evaporations while the slide was still cold.

For the methyl-isocyanide-doped junctions, the rhodium and iron particles were evaporated in vacuum of order 10^{-6} Pa or in CO (at pressures of order 7×10^{-5} Pa). After being warmed up to room temperature, the junction was doped with methyl isocyanide vapor at a pressure of 3×10^{-5} Pa for 30 s and completed by the evaporation of the top electrode 2000–3000 Å thick. The methyl isocyanide was prepared according to the literature³² and kept at -80 °C except during doping when the compound was warmed up to a temperature of order 5 – 10 °C.

We fabricated junctions in pairs, one with metal particles and the other without. Both junctions had the same exposure to the compounds. The spectra of the junctions without the metal particles had no peaks due to the compound. Neither CO nor CH_3NC bonded to alumina under our experimental conditions.

To minimize the background features, we used a

differential spectrometer to subtract the spectrum of the control junctions from the doped one.³³ We used the method of mean intercepts to measure the peak position.³⁴

III. RESULTS AND DISCUSSION

Figure 1 shows a transmission electron micrograph of rhodium-alumina surface. The picture is reproduced from Ref. 13. For this sample the total mass of the deposited rhodium as measured by a quartz crystal is equivalent to a 4-Å-thick continuous layer. The large crystalline structure is the polycrystalline aluminum film. The aluminum oxide is too thin (on the order of 20 Å thick) to be seen. The small spots covering the entire photograph are the rhodium particles with average size near 25 Å. For our samples, the mass of the deposited rhodium is equivalent to a 3-Å-thick continuous layer. Hence, we may expect the average particle size to be smaller. Figure 2 is a sketch of what the cross section of a tunnel junction containing rhodium particles may look like.

We were not able to resolve any structure on the electron micrograph pictures for the iron particle samples. The total mass of the deposited iron is equivalent to a 1-Å-thick continuous layer. To obtain spectra without large background structure³⁵ and zero-bias anomalies,³⁶ we kept the particle size small by (1) evaporating small amounts of metal, and (2) keeping the substrate chilled during evaporation.

Figure 3 shows examples of differential tunneling spectra of CO bonded to Fe with In and Pb top metal electrodes. Kroeker *et al.*³⁷ have shown that with a Pb top electrode the peaks at 54.1 and 64.6 meV are

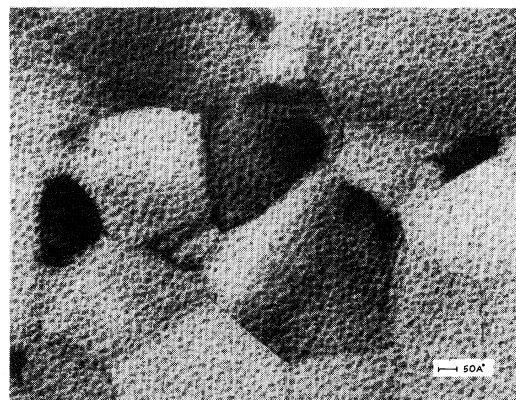


FIG. 1. The electron micrograph shows rhodium particles with an average diameter of 25 Å. The sample is prepared on a carbon-coated nickel grid. The relatively large crystallites are in the aluminum film which is deposited on the grid and oxidized as in the preparation of a tunneling junction.

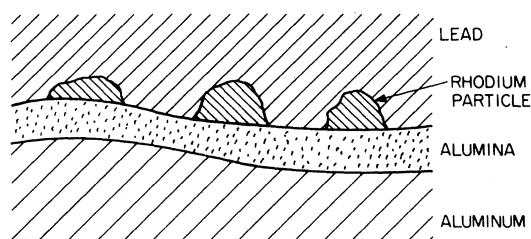


FIG. 2. Cross-sectional sketch of the oxide interface in a tunnel junction containing metal particles. The particle size and distribution of particles are based on the micrograph of Fig. 1. We do not, however, know the contact angle between the rhodium particles and the alumina surface.

bending modes and the peak at 70.6 meV is a stretching mode. The peak at 230.1 meV is the CO stretching vibration. In Fig. 4, we present the differential spectra of junctions with different top metal electrodes, where the regions of interest are expanded. We observe that in the low-energy region the spectra show similarities in pairs of atoms with similar radii: Pb (1.745 Å) and Tl (1.71 Å), Sn (1.582 Å) and In (1.57 Å), Ag (1.442 Å) and Au (1.439 Å).³⁸ Large differences in atomic radii give qualitative differences in spectra. Looking at Table I we can see that within pairs, the peak positions are, in general, at lower frequencies for the smaller top metal atom. The peak position for the CO stretching vibration moves to lower frequencies going from Pb to Au.

Figure 5 shows expanded differential spectra of vibrational modes due to CO on Rh. The isotope studies of the modes with Pb top electrode suggest that the main contribution to the modes at 51.2 and 56.0 meV are the bending vibrations due to two different

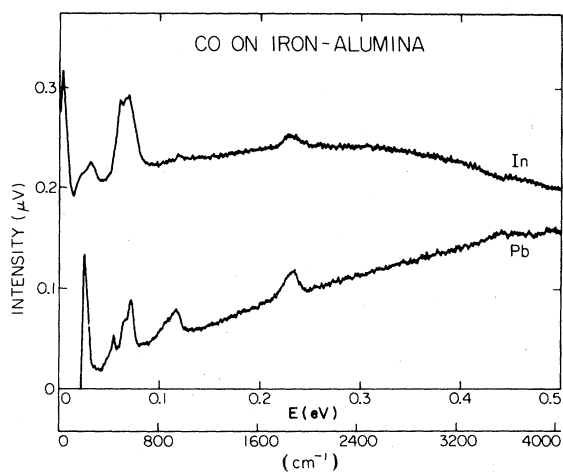


FIG. 3. Differential tunneling spectra of CO on Fe alumina with In and Pb top metal electrodes. In the Pb spectrum the peaks at 25 and 116 meV are due to the superconducting Pb electrode and alumina support, respectively.

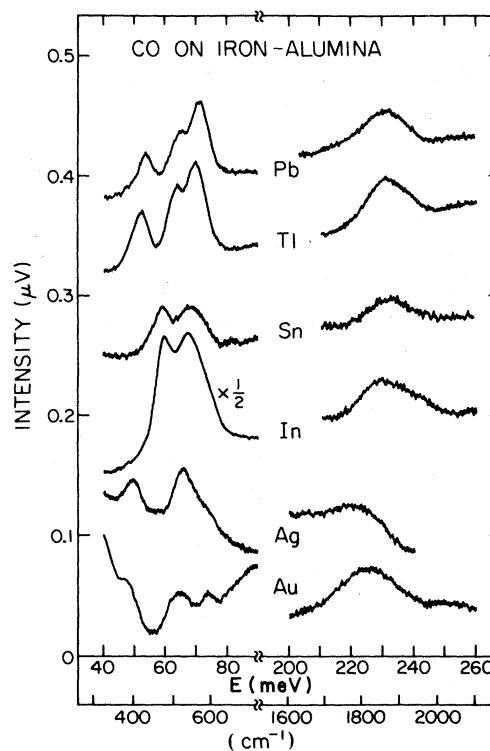


FIG. 4. Differential spectra of CO bonded to Fe with different top metal electrodes showing the low-energy region and the CO stretching bands.

linear species and at 70.8 meV are bending vibrations due to bridged species. The modes at 214.6 and 241.9 meV are CO stretching vibrations due to bridged and linear species, respectively. Figure 5 also includes the spectrum with normal Pb top electrode. The peaks are slightly broader and some are downshifted compared to the Pb superconducting spectrum. Since the other metals used are not superconducting, they should be compared to the normal Pb spectrum. The results for CO on Rh follow the results for CO on Fe: Pb and Tl, Sn and In give similar spectra in pairs. The peak positions for Tl and In are downshifted from Pb and Sn, respectively (see Table II).

Figure 6³⁹ shows the tunneling and infrared spectra of methyl isocyanide bonded to alumina supported rhodium. The peak positions for the CH₃ bending and stretching vibrations compare well to those found by infrared measurements without a top electrode (see Table III). The tunneling spectrum extends to lower energies where the observed peaks probably correspond to *M*-C-N bending and stretching vibrations where *M* represents the metal involved. (We have not identified these peaks with isotopic shift measurements.) The striking comparison is in the 250–300-meV region where there is a dip (280 meV) in the tunneling spectrum whereas the infrared spec-

TABLE I. CO on iron-alumina with different top electrodes. Peak positions are given in meV. To convert to cm^{-1} multiply by 8.065.

Pb	Tl	Sn	In	Ag	Au
54.1 ± 0.1	52.4 ± 0.2			49.5 ± 0.2	48.8 ± 0.4
64.4 ± 0.1	62.9 ± 0.3	59.2 ± 0.1	60.5 ± 0.4	65.2 ± 0.3	64.4 ± 0.7
70.6 ± 0.2	69.7 ± 0.2	68.4 ± 0.4	67.6 ± 0.2		73.7 ± 0.4
230.1 ± 0.4	230.1 ± 0.6	231.1 ± 0.3	229.4 ± 0.8	224.7 ± 0.7	225.3 ± 0.5

trum has its most intense absorption peak (275 meV). The peak is identified as the $-\text{N} \equiv \text{C}$ stretching vibration with the carbon bonded to the surface.

Why has not the dip been seen before? Is something special about the $-\text{N} \equiv \text{C}$ stretching vibration? It has a large dipole derivative. Carbon monoxide also has a large dipole derivative and we have been puzzled by the unusually small intensities we see for the CO stretching vibration in our tunneling spectra. Is the same physics responsible for both effects? On the other hand, strong $\text{C} \equiv \text{N}$ vibrations have been observed in tunneling spectra. Mazur and Hipps⁴⁰ doped their junctions with water solutions of KNCS, KOCN, and KCN. Though they observed no peaks for the cyanide ion (i.e., no peaks due to $\text{Al}-\text{CN}$ structure), the spectrum of junctions doped with thiocyanate (NCS^-) and isocyanate (OCN^-) ions show sharp, intense CN bending and stretching vibra-

tions mainly due to the $\text{Al}-\text{NCS}$ and $\text{Al}-\text{OCN}$ structures, respectively.

In an attempt to answer these questions, we studied the asymmetry of the spectra and the sensitivity of the dip to the tunnel junction environment. In Fig. 7, we present the forward and reverse biased spectra of the first and second harmonic signals from a junction with rhodium particles and doped with methyl isocyanide. The second harmonic spectrum shows an antisymmetry in the region of the dip.

Figure 8 compares the tunneling spectra of the junctions doped with methyl isocyanide and completed with different top metal electrodes—Pb, Tl, and Sn. There are no detectable shifts for the peaks at 121.5, 139.0, and 370 meV (see Table III). Changes occur in the low energy, CH_3 bending, 250–300 meV regions. Going from lead to tin the CH_3 bending region loses resolution.

The intense peak at 60 meV in the spectrum of the junction with the Pb top electrode is greatly reduced in intensity in the spectrum of the Tl top electrode junction. In the case of Sn, there is no appreciable peak at that energy. A similar trend is observed for the dip. For the Pb top electrode, there is a slight rise in the background after 250 meV and an intense dip at 279–280 meV. For the Tl top electrode the structure looks like a peak followed by a dip of equal intensity. When Sn is used as the top metal electrode a broad weak peak at 267 meV is observed. There is

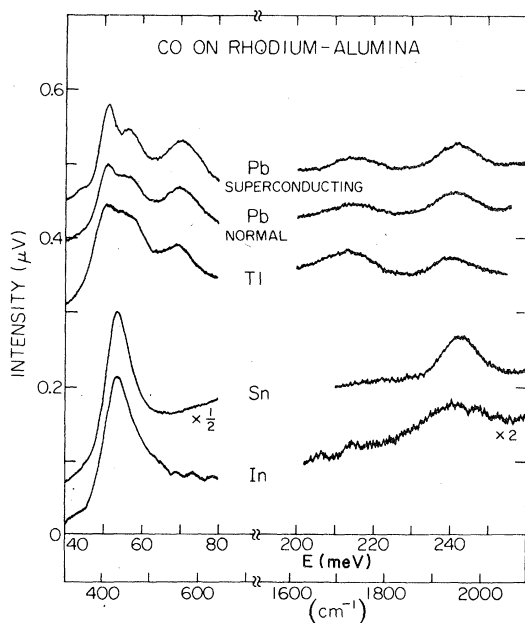


FIG. 5. Differential spectra of CO bonded to Rh with different top metal electrodes.

TABLE II. CO on rhodium-alumina with different top electrodes. Peak positions are given in meV.

Pb(s) ^a	Pb(n) ^b	Tl	Sn	In
51.2	50.6	51.0	53.5	53.4
56.9	56.9	57.6		
70.8	69.9	69.9		
214.8	214.4	213.5		
241.9	241.2	240.0	242.7	240.7

^aPb is superconducting.

^bPb is normal.

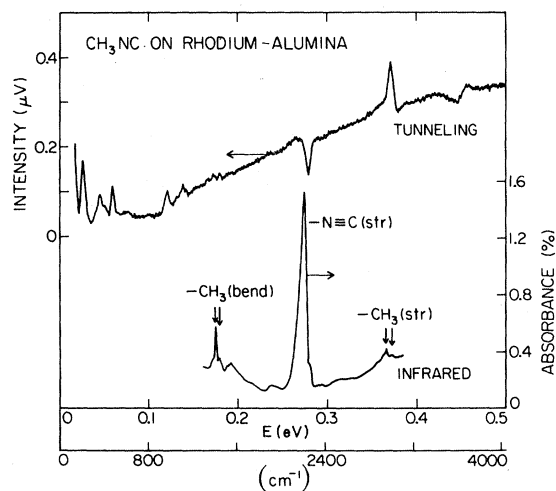


FIG. 6. Spectra of methyl isocyanide bonded to alumina supported rhodium. The tunneling intensities in the top curve are read off the left vertical axis. The infrared absorbance is read off the right vertical axis. Notice the dip in the tunneling spectrum where the infrared spectrum has an intense peak due to $-\text{N}\equiv\text{C}$ stretching vibration. The structure at ~ 450 meV is due to subtraction of a shifted O-H vibration. The infrared spectrum is by Cavanagh and Yates (Ref. 39).

still an indication of a dip following the peak.

Preliminary comparison with existing theories of tunneling spectroscopy is useful. Davis²⁴ has calculated antisymmetric logarithmic singularities and symmetric step-function decreases in the conductance for the elastic tunneling channel. These terms are due to an interference between the direct elastic tunneling process and a two-step process involving the virtual excitation and deexcitation of the vibrator. The contribution to the conductance of these second-order terms is appreciable only when the interaction poten-

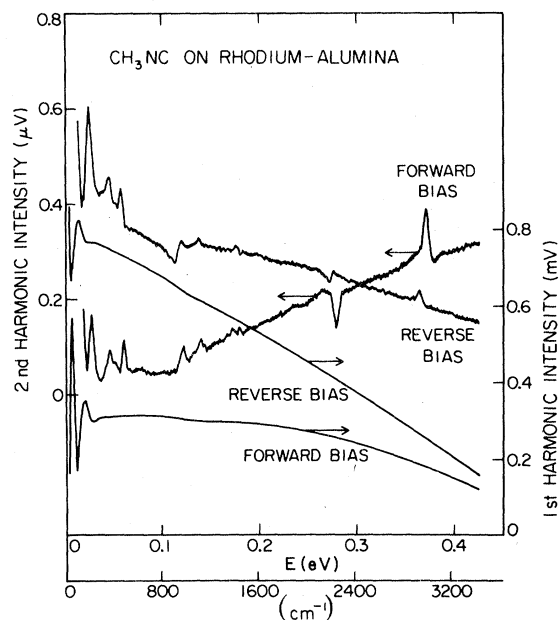


FIG. 7. First and second harmonic intensities for methyl isocyanide on rhodium on alumina. The forward bias curves are due to tunneling from aluminum to lead (aluminum negatively biased) and for the reverse bias curves the tunneling is in the opposite direction. The first harmonic curves (proportional to dV/dI) are offset: the forward biased curve by 1.6 mV and reverse bias curve by 1.1 mV.

tial is large near the metal electrodes. Hence, if the oscillator is buried well into the barrier, the second-order terms are negligible. Birkner and Schattke²⁸ who studied the variation of the conductance with the position of the impurity for finite temperatures in a renormalized perturbation treatment also found that the anomalous behavior is strongest when the oscillator is right at the interface. Why then is the dip

TABLE III. Methyl isocyanide on supported metals. Peak positions are given in meV.

Infrared for Rh-alumina	Tunneling for Rh-alumina			Tunneling for Fe-alumina Pb
	Pb	Tl	Sn	
	46.0	46	48	48
	50.0		55	
	59.5	60		60.5
	121.5	120	120	121.0
	139.0	138	139	139.7
175.4	173.0	172		171.1
179.5	180.0	179	178	179.5
	190.0			
274.5	280.0 dip	277 dip	267	258.2
356.8				362.4
372.3	370.0	370	370	368.8

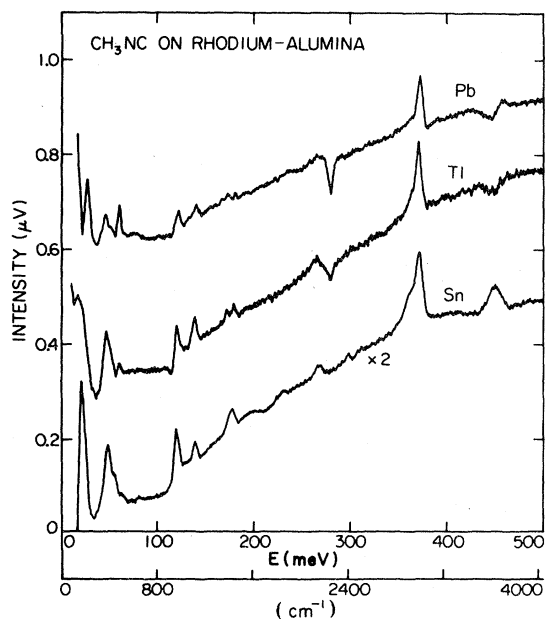


FIG. 8. Differential tunneling spectra of methyl isocyanide adsorbed on rhodium particles supported by alumina. Each spectrum is of a junction completed with a different top metal electrode. The metal-carbon vibrations as well as the dip are sensitive to the top metal electrode.

smaller for electrodes such as Sn which are believed to be effectively closer to the oscillators they cover? Perhaps it is the combination of the metal particles and the top electrode that is important. The spectrum of methyl isocyanide bonded to iron particles is shown in Fig. 9. The spectrum is very similar to the spectrum of the compound bonded to rhodium particles except the $-\text{N}\equiv\text{C}$ vibration is observed at 258 meV as a small broad peak. It is clear from our experiments that the dip is extremely sensitive to the local environment.

What is the effect of the metal particles contained in the tunneling barrier on the tunneling line shapes? Zeller and Giaever⁴¹ have shown that the radius of particles that are included on a tunneling barrier and are insulated from both metal films can be estimated from the electrical characteristics near $V=0$. For 30-Å particles the characteristic width of the resistance peak near $V=0$ at 4.2 K is of order 40 meV. We do not observe any measurable anomaly on that voltage scale. This is not surprising since the metal particles in our experiments were not oxidized and thus may not be insulated from top metal film. Thus, the particular two step process considered by Zeller and Giaever probably is not important in our experiments. We also do not find evidence for the magnetic anomaly discussed by Wolf⁴² in our experiments. However, a two step process may be important in understanding the dip.

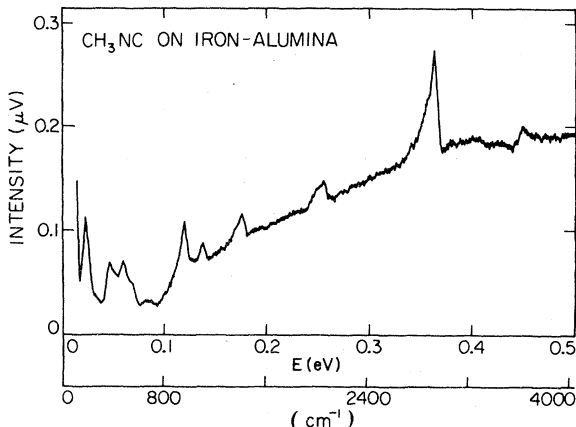


FIG. 9. Differential tunneling spectrum of methyl isocyanide adsorbed on iron particles supported by alumina. Lead is used as the top metal electrode.

Other general theories of tunneling spectroscopy²⁵⁻²⁷ may also be useful in explaining the effect. These theories have not yet, however, been worked out in sufficient detail to predict under what conditions dips or other peak shapes should be expected. We look forward to further developments.

IV. SUMMARY

Though the tunnel junction environment is often surprisingly benign, under some circumstances it can have a major effect on tunneling spectra:

(1) The top metal electrode dramatically affects the vibrational mode energies of CO bonded to transition metals: Atoms with similar radii give similar spectra, while atoms with dissimilar radii give qualitatively different spectra.

(2) Though, in general, intense peaks in optical spectra correspond to intense peaks in tunneling spectra; in the case of the $-\text{N}\equiv\text{C}$ stretching mode of methyl isocyanide on Rh an intense peak in the infrared spectrum correspond to a *dip* in the tunneling spectrum.

(3) This dip is sensitive both to the metal on which the methyl isocyanide is adsorbed and to the top metal electrode.

(4) In agreement with previous measurements, the vibrational modes of an adsorbed hydrocarbon group are shifted by the top metal electrode by less than 1% from the values found by infrared spectroscopy.

ACKNOWLEDGMENTS

We thank John T. Yates, D. J. Scalapino, and Richard M. Kroeker for useful suggestions. This work was partially supported by the Division of Materials Research of the National Science Foundation (DMR79-25430) and the Office of Naval Research.

- ¹W. H. Weinberg, *Annu. Rev. Phys. Chem.* **29**, 115 (1978).
²P. K. Hansma, *Phys. Rep.* **30**, 145 (1977).
³R. C. Jacklevic and J. Lambe, *Phys. Rev. Lett.* **17**, 1139 (1966).
⁴H. W. White, L. M. Godwin, and T. Wolfram, *J. Adhes.* **9**, 237 (1978).
⁵A. F. Diaz, U. Hetzler, and E. Kay, *J. Am. Chem. Soc.* **99**, 6780 (1977).
⁶D. N. Henrickson, H. T. Chu, N. K. Eib, and A. N. Gent, *Adv. Chem. Ser.* **174**, 87 (1979).
⁷P. K. Hansma and R. V. Coleman, *Science* **184**, 1369 (1974).
⁸P. A. Cass, H. L. Strauss, and P. K. Hansma, *Science* **192**, 1128 (1976).
⁹Y. Skarlatos, R. C. Barker, and G. L. Haller, *Surf. Sci.* **43**, 353 (1974).
¹⁰J. T. Hall, P. K. Hansma, and M. Parikh, *Surf. Sci.* **65**, 552 (1977).
¹¹J. M. Clark and R. V. Coleman (unpublished).
¹²A. Bayman and P. K. Hansma, *Nature (London)* **285**, 97 (1980).
¹³R. M. Kroeker, W. C. Kaska, and P. K. Hansma, *J. Catal.* **57**, 72 (1979).
¹⁴H. E. Evans and W. H. Weinberg, *J. Chem. Phys.* **71**, 1537 (1979).
¹⁵H. E. Evans, W. M. Bowser, and W. H. Weinberg, *Surf. Sci.* **85**, L497 (1979).
¹⁶R. M. Kroeker, W. C. Kaska, and P. K. Hansma, *J. Catal.* **61**, 87 (1980).
¹⁷J. R. Kirtley and P. K. Hansma, *Phys. Rev. B* **12**, 531 (1975).
¹⁸J. R. Kirtley and P. K. Hansma, *Phys. Rev. B* **13**, 2910 (1976).
¹⁹D. J. Scalapino and S. M. Marcus, *Phys. Rev. Lett.* **18**, 459 (1968).
²⁰J. Lambe and R. C. Jacklevic, *Phys. Rev.* **165**, 821 (1968).
²¹A. J. Bennet, C. B. Duke, and S. D. Silverstein, *Phys. Rev.* **176**, 969 (1968).
²²J. Kirtley, D. J. Scalapino, and P. K. Hansma, *Phys. Rev. B* **14**, 3177 (1976).
²³A. D. Brailsford and L. C. Davis, *Phys. Rev. B* **2**, 2910 (1970).
²⁴L. C. Davis, *Phys. Rev. B* **2**, 1714 (1970).
²⁵C. Caroli, R. Combescot, P. Nozières, and D. Saint-James, *J. Phys. C* **5**, 21 (1972); **4**, 916 (1971).
²⁶C. B. Duke, G. G. Kleinman, and T. E. Stakelon, *Phys. Rev. B* **6**, 2389 (1972).
²⁷T. E. Feuchtwang, *Phys. Rev. B* **13**, 517 (1976); **10**, 4135 (1974); **10**, 4121 (1974).
²⁸G. K. Birkner and W. Schattke, *Z. Phys.* **256**, 185 (1972).
²⁹J. Kirtley and J. T. Hall, *Surf. Sci.* (in press).
³⁰J. Kirtley and P. K. Hansma, *Surf. Sci.* **66**, 125 (1977).
³¹K. Magno and J. G. Adler, *Phys. Rev. B* **13**, 2262 (1976).
³²J. Casanova, Jr., R. E. Schuster, and N. D. Werner, *J. Chem. Soc.* 4280 (1963).
³³P. K. Hansma and J. R. Kirtley, *Acc. Chem. Res.* **11**, 440 (1978).
³⁴P. S. Braterman, *Metal Carbonyl Spectra* (Academic, New York, 1975), Chap. 5.
³⁵J. R. Cooper and A. F. Wyatt, *J. Phys. F* **3**, L120 (1973).
³⁶E. L. Wolf, *Rep. Prog. Phys.* **41**, 1439 (1978).
³⁷R. M. Kroeker, P. K. Hansma, and W. C. Kaska, *J. Chem. Phys.* **72**, 4845 (1980).
³⁸*American Institute of Physics Handbook*, 3rd ed., edited by D. E. Gray (McGraw-Hill, New York, 1972), p. 7.
³⁹R. R. Cavanagh and J. T. Yates, Jr., *Surf. Sci.* **99**, L381 (1980).
⁴⁰U. Mazur and K. W. Hipps, *J. Phys. Chem.* **83**, 2773 (1979).
⁴¹H. R. Zeller and I. Giaever, *Phys. Rev.* **181**, 789 (1969).
⁴²E. L. Wolf, *Solid State Phys.* **30**, 1 (1975).

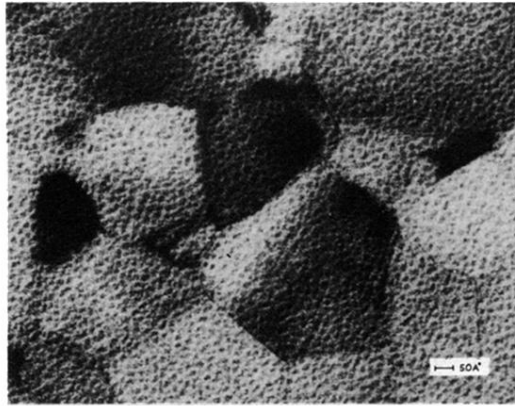


FIG. 1. The electron micrograph shows rhodium particles with an average diameter of 25 Å. The sample is prepared on a carbon-coated nickel grid. The relatively large crystallites are in the aluminum film which is deposited on the grid and oxidized as in the preparation of a tunneling junction.